Published in final edited form as:

Nature. 2001 October 11; 413(6856): 603–609. doi:10.1038/35098027.

A sperm ion channel required for sperm motility and male fertility

Dejian Ren[*], **Betsy Navarro**[*], **Gloria Perez**[†], **Alexander C. Jackson**[*], **Shyuefang Hsu**[*], **Qing Shi**[*], **Jonathan L. Tilly**[†], **David E. Clapham**[*]

[*]Howard Hughes Medical Institute, Children's Hospital, Harvard Medical School, Enders 1309, 320 Longwood Avenue, Boston, Massachusetts 02115, USA

[†]Vincent Center for Reproductive Biology, Massachusetts General Hospital and Department of Obstetrics, Gynecology and Reproductive Biology, Harvard Medical School, Boston, Massachusetts 02114, USA

Abstract

Calcium and cyclic nucleotides have crucial roles in mammalian fertilization, but the molecules comprising the Ca^{2+}-permeation pathway in sperm motility are poorly understood. Here we describe a putative sperm cation channel, CatSper, whose amino-acid sequence most closely resembles a single, six-transmembrane-spanning repeat of the voltage-dependent Ca^{2+}-channel four-repeat structure. CatSper is located specifically in the principal piece of the sperm tail. Targeted disruption of the gene results in male sterility in otherwise normal mice. Sperm motility is decreased markedly in CatSper$^{-/-}$ mice, and CatSper$^{-/-}$ sperm are unable to fertilize intact eggs. In addition, the cyclic-AMP-induced Ca^{2+} influx is abolished in the sperm of mutant mice. CatSper is thus vital to cAMP-mediated Ca^{2+} influx in sperm, sperm motility and fertilization. CatSper represents an excellent target for non-hormonal contraceptives for both men and women.

Male sperm and female eggs interact reciprocally in mammalian fertilization[1,2]. To reach the site of fertilization, sperm must travel long distances and become primed for fertilization of the eggs through capacitation and other processes. Once they arrive at the surface of the egg, sperm interact with the egg's extracellular matrix glycoproteins including the zona pellucida proteins. Sperm release acidic material during the acrosome reaction, a signalling event that presumably involves the opening of Ca^{2+} channels and the influx of Ca^{2+} into the sperm heads[3]. Transient receptor potential protein channel 2 (TRPC2), a putative Ca^{2+}-permeant channel, has been implicated in the acrosome reaction[4]. Penetration of sperm through the thick outer layer of the egg is achieved through chemical lysis of the egg coat and/or the mechanical motion of sperm[5]. After infiltrating the egg's zona pellucida coat, the sperm membrane fuses with that of the egg. Fusion is followed by activation of the fertilization process, beginning with Ca^{2+} oscillations in the egg[1,2].

Ca^{2+} and cyclic nucleotides control sperm motility[6–8] and several voltage-dependent Ca^{2+}-channel (Ca_V) messenger RNAs and cyclic-nucleotide-gated (CNG) proteins

Correspondence and requests for materials should be addressed to D.E.C. (dclapham@rascal.med.harvard.edu). The GenBank accession numbers are AF407332 for mouse CatSper and AF407333 for human CatSper.

have been detected in sperm cell precursors[7,9–11]. Furthermore, low-voltage-activated, dihydropyridine-sensitive “T-type” channels[12,13] and pharmacologically defined N- and R-type currents have been measured in spermatogenic cells[14]. But the role of these channels in spermatogenesis or mature sperm function is not known.

Here we describe the cloning and functional characterization of an unusual sperm cation channel. The CatSper gene is unique in that it encodes a single, six-transmembrane-spanning repeat (like voltage-dependent K^+ (K_V) channels), but its pore region and overall homology is closest to a single domain of the much larger four-repeat Ca_V channels. The gene product is expressed exclusively in the testis and not in other tissues such as the brain, heart, kidney or immune system. In sperm, the channel is localized primarily to the tail’s principal piece, not the head or midpiece. As we show, poor sperm motility and male infertility result from gene-targeted elimination of the mouse CatSper protein.

Cloning of the putative one-repeat cation channel CatSper

While searching for Ca^{2+} channels, we discovered a fragment of an expressed sequence tag (EST) complementary DNA (accession number AA416682) that showed similarity to known voltage-gated Ca^{2+} channels. Expression analysis showed that it was present only in testis (see below). Polymerase chain reaction (PCR) and library screening were used to clone the full-length cDNAs from human and mouse testis. The gene for CatSper (cation channel of sperm) predicted a primary structure of 686 amino acids (Fig. 1a).

In a BLAST search (see http://www.ncbi.nlm.nih.gov), the functional proteins with closest similarity to CatSper were voltage-gated Ca^{2+} channels, not K_V, CNG or TRP channels. The pore-forming subunits (α_1) of Ca_V channels have four repeats of a six-transmembrane-spanning domain[15]. Located in the putative channel pore region of each of the four repeats are glutamine/aspartate residues that impart Ca^{2+} selectivity on the channel by coordinating Ca^{2+} ions[16]. These residues are conserved among all the established Ca_V channels and CatSper (Fig. 1c).

As is characteristic for voltage-gated channels, positively charged amino acids (lysine/arginine) are interspersed every three amino acids in the transmembrane region of the putative CatSper S4 domain. Like K_V, CNG and TRP channels, a hydrophobicity plot of CatSper (Fig. 1b) predicted that it contained six-transmembrane-spanning domains. CatSper contains a remarkable abundance of histidine residues in its amino terminus (49/250 amino acids), which might be involved in the well-known pH regulation of sperm motility[2]. Human CatSper exhibits a high degree of homology (55% identity/72% similarity) with its mouse counterpart, especially in the transmembrane domains and the histidine-rich region. The transmembrane domains share 81% identity/93% similarity, and the pore region shares 89% identity/100% similarity. Low stringency screening of a mouse testis cDNA library with human CatSper detected no genes of higher similarity.

CatSper is localized to the principal piece

CatSper messenger RNA was detected in testis as a single band of roughly 2.6 kilobases. The size of the mRNA was similar to that of the cDNA clones that we isolated, suggesting

that the gene product was a full-length transcript and not a truncated form of a much larger conventional Ca_V channel. CatSper mRNA was not detected in any of 8 mouse or 16 human organs, including brain, heart, spleen, lung and skeletal muscle (Fig. 2a). Furthermore, a CatSper mRNA probe recognized only testis in a dot blot of 50 human tissue mRNAs (Fig. 2b).

A polyclonal antibody directed against the first 150 amino acids of the amino terminus recognized CatSper protein (Fig. 2c). The antibody specifically labelled tetracycline-induced CatSper proteins from HEK-293 cells and native CatSper in testis, sperm (Fig. 2c) and spermatocytes. Consistent with the results of the northern blots, the antibody did not recognize similar size proteins from brain, heart or kidney (data not shown).

We used indirect immunofluorescence to determine the subcellular localization of sperm CatSper. The protein was highly localized to the principal piece of the sperm tail (Fig. 3a). CatSper was presumably localized to the plasma membrane because the principal piece does not contain intracellular organelles (such as endoplasmic reticulum). To determine the precise location of the protein in the sperm tail, we performed indirect immunogold electron microscopy. CatSper immunoreactive gold particles were detected in the plasma membrane above the fibrous sheath in the sperm principal piece (Fig. 3b). Consistent with the immunoflorescence staining, few immunoreactive gold particles were detected in either the head or midpiece. The detection of gold particles on the cytoplasmic face of the plasma membrane (Fig. 3b, middle) supports the predicted intracellular localization of the N terminus of CatSper.

Targeted disruption of CatSper

We disrupted CatSper in embryonic stem cells by homologous recombination to study its function *in vivo* (Fig. 4a). The second exon encoding the first putative transmembrane domain was replaced with an IRES–LacZ sequence followed by the neomycin resistance gene.

To generate chimaeras, embryonic stem cells carrying a mutant copy of the gene were injected into blastocysts and implanted in pseudo-pregnant mice. Mutant mice were generated from the mating of offspring. Disruption of the gene was confirmed by polymerase chain reaction (PCR) (Fig. 4b), western blotting (Fig. 4c), immunostaining (Fig. 4d) and immunogold electron microscopy (data not shown).

CatSper is required for male fertility

The genotypes of heterozygous (+/−) male and female offspring exhibited roughly mendelian proportions (240 heterozygous, 106 wild-type and 110 mutant), suggesting that the mutation did not affect embryonic development. $CatSper^{-/-}$ (mutant) mice were indistinguishable from their wild-type littermates in survival rates, appearance and gross behaviour.

Homozygous (−/−) females mated with heterozygous (+/−) or wild-type (+/+) males were fertile. Homozygous male mutants mated with wild-type females displayed mounting

behaviour indistinguishable from that of wild-type males. The similar frequencies of vaginal plugs noted in mated females supported the normal mating behaviour of wild-type and mutant mice. However, the mutant males engendered no pregnancies over a period longer than 2 months (up to 9months, $n = 26$ females, $n = 13$ males). In contrast, the wild-type littermate males were 100% fertile ($n = 8$ females, $n = 4$ males; Fig. 5a).

Body and testis weights of the mutant mice were not different from those of their wild-type counterparts (Fig. 5b). Sperm counts from mutant and wild-type caudal epididymis were not significantly different, and the sperm were cytologically indistinguishable (Fig. 5c). The absence of spermatogenesis defects in CatSper$^{-/-}$ mice was supported by the lack of morphological differences between wild-type and mutant mouse testes (Fig. 5d).

A major effort was made to determine the precise electrophysiological characteristics of the wild-type and mutant sperm. As detailed below, hundreds of attempts to measure whole-cell currents of both wild-type and mutant sperm under a variety of conditions and configurations were unsuccessful, consistent with the experience of other investigators. But we could record voltage-gated Ca^{2+}-channel currents from mutant and wild-type spermatocytes. The measured Ca^{2+} currents were consistent with previous data[12,13], and no significant differences between wild-type and mutant mouse spermatocyte inward currents were detected (Fig. 5e). No inward currents were induced by cyclic nucleotides in wild-type or mutant spermatocytes (data not shown). Thus, CatSper is not a main component of the spermatocyte voltage-sensitive Ca^{2+} currents and is not required for the development of sperm from spermatocytes.

CatSper is required for normal sperm motility

A closer examination of live sperm under light microscopy revealed a significant difference between the mutant and wild-type sperm. Sperm from wild-type mice displayed vigorous beating in the tail region and progressive directed movement. By contrast, CatSper$^{-/-}$ sperm were sluggish and displayed less directed movements.

Most notably, mutant sperm lacked the vigorous beating and bending in the tail region. Computer-assisted sperm analysis showed that the mutant sperm's main motility parameters of path velocity, progressive velocity and track speed were impaired significantly (Fig. 6a). Thus, disrupting the CatSper gene results in markedly reduced sperm motility.

CatSper is required to penetrate the egg

In vitro fertilization (IVF) assays were performed to test CatSper$^{-/-}$ sperm's ability to fertilize eggs. Superovulated wild-type female mature eggs incubated with capacitated wild-type or mutant sperm were examined after 24 h. The appearance of two-cell-stage embryos was taken to indicate successful penetration of sperm and subsequent activation of fertilization. Whereas 81% of eggs (66/81) were fertilized by wild-type sperm, no eggs (0/79) were fertilized by CatSper$^{-/-}$ sperm (Fig. 6b). The eggs fertilized by wild-type sperm developed into two-cell-stage embryos, but those incubated with mutant sperm remained at the single-cell stage (Fig. 6c). Some CatSper$^{-/-}$ sperm adhered to the eggs but did not seem to be able to penetrate the eggs, possibly owing to impaired motility.

During the course of natural fertilization, sperm penetrate the surrounding layer of zona pellucida proteins and fuse to the egg's plasma membrane. To examine whether the mutant sperm retained the ability to fuse with the plasma membrane and activate fertilization, we incubated wild-type and mutant sperm with eggs whose outer layers had been enzymatically removed (zona-pellucida-free eggs). Under such conditions, sperm from both CatSper$^{+/+}$ and CatSper$^{-/-}$ mice were capable of fertilizing the eggs (Fig. 6b, c). Thus, we conclude that CatSper is required for the sperm to be able to penetrate the egg outer layers, but not for egg activation.

CatSper is required for cAMP-induced Ca^{2+} influx

Cyclic nucleotides have been widely implicated in sperm motility[6–8,17]. To elucidate the function of CatSper, we expressed mouse and human CatSper in various heterologous expression systems including *Xenopus* oocytes, and HEK-293 and CHO-K1 cells. In over 250 patch-clamp studies, we failed to detect a significant current resulting from CatSper expression, alone or in combination with expressed CNG β-channel subunits (CNG4 or CNG6). Although CatSper protein was detected in the expression system (Fig. 2c), no currents could be elicited by changes in voltage, pH, osmolarity and/orcyclic nucleotide concentration. As a positive control, we measured cyclic-nucleotide-activated channel currents after expression of the CNG a-subunit (CNG1) and β-subunit (CNG6).

We also attempted to compare the currents of wild-type and mutant sperm head and tail membranes. As reported by others[18], the success rate for obtaining stable patches from sperm was very low, presumably owing to the small diameter (0.5 μm) and the geometry of sperm tails. Out of about 900 attempts under various conditions, less than 30 gigaseals were formed and none was a stable whole-cell recording. Although no differences between wild-type and mutant cell-attached patches were noted, the low success rate prevented any reliable analysis. We therefore chose to examine sperm tail intracellular Ca^{2+} dynamics, which can be readily monitored with Ca^{2+} indicators[11,19].

We loaded wild-type and mutant sperm with Fluo-4, and measured their fluorescence by single-photon confocal microscopy. Application of cell-membrane-permeant cAMP (1mM 8-Br-cAMP) to the bath solution containing caudal epididymal wild-type sperm initiated a rapid rise in sperm head and tail intracellular calcium concentration ($[Ca^{2+}]_i$) (Figs 7a, b, and 8). This $[Ca^{2+}]_i$ signal was not detected in Ca^{2+}-free bath medium (data not shown), suggesting that the Ca^{2+} influx was mediated by a plasma membrane channel. Membrane-permeant cGMP (1mM 8-Br-cGMP) also initiated Ca^{2+} influx in sperm. The cAMP- and cGMP-induced $[Ca^{2+}]_i$ increase was not blocked by incubating sperm with the nonspecific kinase inhibitor staurosporine (1 μM, 10 min), suggesting that cyclic-nucleotide-dependent protein kinases are not essential for channel activation.

Adding sodium bicarbonate (20 mM), a physiologically relevant stimulus to sperm[8], to the bath induced an increase in $[Ca^{2+}]_i$ that was smaller than that observed with cAMP or cGMP (data not shown). A significant cyclic-nucleotide-induced $[Ca^{2+}]_i$ rise was also detected in testis-derived sperm but not in spermatids (nor in developing elongated spermatids with short tails; data not shown), suggesting that the Ca^{2+} response to cAMP is a property

of the fully differentiated sperm. In CatSper$^{-/-}$ sperm, neither cAMP nor cGMP elicited a significant Ca^{2+} influx (Figs 7d, e, and 8). As a control for sufficient dye loading, progesterone initiated a large Ca^{2+} influx in both mutant (Fig. 7f) and wild-type sperm. We conclude that CatSper is required for the cAMP- and cGMP-induced Ca^{2+} influx in sperm.

Discussion

We have cloned a six-transmembrane-spanning putative cation channel, CatSper, that is restricted predominantly or completely to the principal piece of the sperm tail. This putative channel is required for male fertility in mice. CatSper mRNA and protein is present only in testis; immunocytochemistry localized CatSper specifically to the principal piece of mature sperm, and immunogold labelling showed that it is associated primarily with the plasma membrane. The complete lack of intracellular organelles in the principal piece suggests that CatSper cannot be an intracellular channel.

CatSper$^{-/-}$ sperm are poorly motile and unable to fertilize eggs with an intact zona pellucida, but can fertilize eggs in which this membrane has been removed. Finally, on the basis of confocal microscopic measures of Ca^{2+} influx, CatSper is required for cyclic-nucleotide-mediated Ca^{2+} entry in the sperm tail. Taking these observations together, we propose that CatSper is a unique cation channel protein required for normal sperm motility and, in particular, for sperm penetration of the zona pellucida.

Although CatSper is expressed in heterologous systems, as revealed by the presence of protein, we were unable to show that the putative channel formed a functional channel in these nonsperm cells. Co-expression of CatSper and the CNG β-subunit, with or without cyclic nucleotide second messengers, did not result in measurable currents. Voltage-gated Ca^{2+} currents appeared normal in CatSper$^{+/+}$ and CatSper$^{-/-}$ spermatocytes, and CatSper protein did not contribute measurable inward or outward currents stimulated by voltage, pH changes, cyclic nucleotides or osmotic changes. In mature sperm, CatSper protein was localized to the principal piece of the sperm tail—an area that is inaccessible to current patch-clamp methodologies. However, Ca^{2+} imaging of mature sperm from normal and mutant mice revealed that the protein is required for cyclic-nucleotide-stimulated Ca^{2+} influx. The simplest interpretation of the data is that CatSper protein comprises all or part of a tetrameric Ca^{2+}-permeant channel that is gated directly or indirectly by cyclic nucleotides.

The failure to express the channels in heterologous systems suggests that accessory proteins in the principal piece of sperm are not present in any of the three expression systems we used. Alternatively, the proteins may be present in heterologous cells or spermatocytes, but might require structural attributes of the principal piece for their functional organization. Given the low abundance of principal piece tissue, direct biochemical approaches to isolate the putative accessory subunit are not currently feasible. Yeast two-hybrid approaches to find accessory proteins have also been unsuccessful. In a preliminary approach to finding potential accessory subunits, sperm-associated cyclic-nucleotide-gated channels were co-expressed with CatSper but did not yield measurable currents. Clearly, innovative approaches will be required to find the constituents of the presumed functional channel complex.

CatSper represents a unique class of putative ion channel proteins. With the pore features of a Ca^{2+}-selective ion channel, a putative voltage-sensitive S4 domain, and the single repeat structure of K_V, CNG, HCN and TRP channels, CatSper may represent an evolutionary transition channel before gene duplication gave rise to the four-repeat structure of Ca_V channels. The activation mechanism for CatSper is solely a matter of speculation. Cyclic nucleotides regulate sperm motility and are themselves dynamically regulated[6]; however, there are no putative cyclic-nucleotide-binding regions in the primary structure of CatSper. If CatSper is not bound directly by nucleotides, then unknown sperm principal-piece-specific accessory subunits might mediate its regulation.

The activation of CatSper mediates a rise in intracellular Ca^{2+} levels in the sperm tail. The rise of Ca^{2+} regulates sperm motility, presumably through the motor proteins of the tail. If Ca^{2+}-sensitive adenylyl cyclases are present in the sperm, Ca^{2+} entry could accelerate the rise of cAMP[2,6,8], thus providing a positive feedback loop that would amplify cyclic-nucleotide signalling. Such a positive feedback loop may be important in the most vigorous sperm tail beating required for the sperm to penetrate the egg outer layers. Whatever the mechanism of activation, the activity of CatSper seems to depend on the specific structure of sperm tails, and the principal piece in particular. Such a hypothesis explains our finding that cyclic nucleotides induce significant Ca^{2+} influx in testis sperm, but not in spermatids that lack a significant tail.

The human CatSper gene is a potential target for male infertility screening and treatment. Human CatSper is also an ideal target for potential contraceptive drugs. As the *in vitro* fertilization results suggest that CatSper$^{-/-}$ sperm cannot fertilize eggs, a specific blocker of CatSper might be effective when taken by either men or women. The restricted localization of CatSper to mature sperm means that a specific blocker should not affect other tissues, and thus side-effects should be low or nonexistent. The normal development and behaviour (including sexual) of the mutant mice supports such a prediction. Finally, as the channel represents a new structure, it may be an excellent target for channel agonists or antagonists.

Methods

Cloning of CatSper

High-voltage-gated Ca^{2+}-channel protein sequences were used to search the EST database. One EST (AA416682) sequence was analysed and found to be similar to voltage-gated Ca^{2+} channels. We used primers derived from this sequence in PCR after reverse transcription of RNA (RT–PCR) to obtain a cDNA fragment. The fragment was used as a probe to localize the main source of expression in testis. We used cDNA library screening and rapid amplification of cDNA ends to clone the cDNAs containing the whole open reading frame (ORF) from human and mouse testes. The start of the ORF was confirmed by an in-frame stop codon upstream of the first ATG. cDNA constructs for expression in mammalian cells were made by PCR using Pfu polymerase. The constructs were sequenced completely and contained no mutations. Northern and dot blots were from Clontech.

Protein methods

Affinity-purified polyclonal antibody was generated against a glutathione *S*-transferase (GST) fusion protein of the N-terminal 150 amino acids. Western blots were carried out with 2 μg ml^{-1} anti-CatSper antibody. Immunostaining with 5 μg ml^{-1} anti-CatSper antibody was detected with a rhodamine-conjugated anti-rabbit secondary antibody. Anti-CatSper (10 μg ml^{-1}) and 10-nm gold-conjugated protein A particles were used in immuno-electron microscopy; 60-nm sections were cut from embedded cells. We used $CatSper^{-/-}$ sperm as controls in all the experiments to confirm the specificity of the antibodies.

Generation of knockout mice

Genomic bacterial artificial chromosomes clones containing the CatSper gene were isolated and analysed by restriction digestion and sequencing. A targeting vector (Fig. 4a) was constructed to contain 5 kb (left arm), IRES–LacZ followed by a Neo-resistance gene (middle), and 1.7 kb followed by TK as a negative selection marker (right arm). Embryonic stem cells derived from 129/SvJ mice were transfected with linearized DNA, selected and analysed for correct targeting. We used correctly targeted embryonic stem cells to generate chimaeric mice, and crossed these mice with C57BL/6J to obtain heterozygous mutants. Mice used in the study were the offspring of crosses between F_1 and/or F_2 generations (129/SvJ/C57BL/6J genetic background). Wild-type littermates were used as controls in the IVF experiments.

In vitro fertilization

Sperm were collected from cauda epididymis and capacitated *in vitro* for 2 h. Eggs were collected from mature wild-type females (~6-weeks old) synchronized with 10 units of PMSG (pregnant mare serum gonadotropin) and 10 units of hCG (human chorionic gonadotropin) 46–48 h and 14 h before collection, respectively. We carried out IVF using standard protocols[20]. Eggs were incubated with roughly 10^5 $CatSper^{+/+}$ or 10^5 $CatSper^{-/-}$ sperm for 4 h at 37°C, and unbound sperm were washed away. After a 20-h incubation at 37°C, eggs were examined for the presence of the two-cell-stage embryos as an indication of successful fertilization. Some embryos were fixed and stained with Hoechst 33342 for imaging immediately after IVF. The zona pellucida was removed by treatment with hyaluronidase (80 $IUml^{-1}$) followed by perfusion in Tyrode's solution for 30–40 s.

Electrophysiology

Spermatocyte preparation and whole-cell current recording were performed essentially as described[12,21]. The pipette solution contained (in mM): 120 Cs^+, 60 glutamic acid, 20 TEA-Cl, 5 $MgCl_2$, 3 Mg-ATP, 10 EGTA, 10 HEPES and 5 D-glucose (pH 7.4). The bath contained (in mM): 135 NaCl, 5 KCl, 10 $CaCl_2$, 10 sodium lactate, 10 sodium pyruvate, 10 glucose and 30 HEPES (pH 7.4).We subtracted leak currents using an online P/4 protocol. Data were filtered at 1 kHz and corrected for junction potentials.

Ca^{2+} imaging

Sperm were prepared in HS medium[14] and loaded with 10 μM Fluo-4-AM and 0.05% Pluronic F-127 for 30min at room temperature. Washed cells were seeded onto Cell-Tak

coated coverslips. Attached motile sperm were imaged in nonconfocal mode to avoid motion-induced fluorescence change artefacts. We used the 488-nm wavelength beam of an argon–krypton laser for excitation, and monitored fluorescence emission at 512nm (Zeiss LSM 410).

Acknowledgements

We thank K. Wickman and W. Pu for advice on embryonic stem cell handling; G. Krapivinsky and X. Wei for assistance with antibody work and confocal microscopy, respectively; M. Ericsson for electron microscopy; H. Florman, D. Babcock, C. Santi and A. Darszon for advice on spermatocyte and sperm preparation; M. Biel and K.-W. Yau for CNG clones; and D. Garbers and T. Quill for helpful discussions and advice. B.N. was supported by Centro Internacional de Fisica, Lab. de Biofisica, Bogota, Columbia. This work was supported by the Howard Hughes Medical Institute.

References

1. Wassarman PM, Jovine L& Litscheer ES Aprofile of fertilization inmammals. Nature Cell Biol. 3, E59–E64 (2001). [PubMed: 11175768]
2. Yanagimachi R in The Physiology of Reproduction (eds Knobill E & Neill JD) 189–315 (Raven, New York, 1994).
3. O'Toole CM, Arnoult C, Darszon A, Steinhardt RA & Florman HM Ca^{2+} entry through store-operated channels in mouse sperm is initiated by egg ZP3 and drives the acrosome reaction. Mol. Biol. Cell 11, 1571–1584 (2000). [PubMed: 10793136]
4. Jungnickel MK,Marrero H, Birnbaumer L, Lemos JR & Florman HM Trp2 regulates entry of Ca^{2+} into mouse sperm triggered by egg ZP3. Nature Cell Biol. 3, 499–502 (2001). [PubMed: 11331878]
5. Bedford JMMammalian fertilization misread? Sperm penetration of the eutherian zona pellucida is unlikely to be a lytic event. Biol. Reprod. 59, 1275–1287 (1998). [PubMed: 9828168]
6. Tash JS in Controls of Sperm Motility: Biological and Clinical Aspects (ed. Gagnon C) 229–240 (CRC, Boca Raton, 1990).
7. Darszon A, Labarca P, Nishigaki T & Espinosa F Ion channels in sperm physiology. Physiol. Rev. 79, 481–510 (1999). [PubMed: 10221988]
8. Hyne RV & Garbers DL Calcium-dependent increase in adenosine 3′,5′-monophosphate and induction of the acrosome reaction in guinea pig spermatozoa. Proc. Natl Acad. Sci. USA 76, 5699–5703 (1979). [PubMed: 93280]
9. Serrano CJ, Trevino CL, Felix R& Darszon A Voltage-dependent Ca^{2+} channel subunit expression and immunolocalization in mouse spermatogenic cells and sperm. FEBS Lett. 462, 171–176 (1999). [PubMed: 10580114]
10. Weyand Iet al.Cloning and functional expression of a cyclic-nucleotide-gated channel from mammalian sperm. Nature368, 859–863 (1994). [PubMed: 7512693]
11. Wiesner Bet al.Cyclic nucleotide-gated channels on the flagellum control Ca^{2+} entry into sperm. J. Cell Biol. 142, 473–484 (1998). [PubMed: 9679145]
12. Santi CM, Darszon A & Hernandez-Cruz A A dihydropyridine-sensitive T-type Ca^{2+} current is the main Ca^{2+} current carrier in mouse primary spermatocytes. Am. J. Physiol. 271, C1583–C1593 (1996). [PubMed: 8944642]
13. Arnoult C, Cardullo RA, Lemos JR & Florman HM Activation of mouse sperm T-type Ca^{2+} channels by adhesion to the egg zona pellucida. Proc. Natl Acad. Sci. USA 93, 13004–13009 (1996). [PubMed: 8917534]
14. Wennemuth G, Westenbroek RE, Xu T, Hille B & Babcock DF CaV2.2 and CaV2.3 (N- and R-type) Ca2+ channels in depolarization-evoked entry of Ca^{2+} into mouse sperm. J. Biol. Chem. 275, 21210–21217 (2000). [PubMed: 10791962]
15. Ertel EAet al.Nomenclature of voltage-gated calcium channels. Neuron25, 533–535 (2000). [PubMed: 10774722]
16. Ellinor PT, Yang J, Sather WA, Zhang JF & Tsien RW Ca^{2+} channel selectivity at a single locus for high-affinity Ca^{2+} interactions. Neuron 15, 1121–1132 (1995). [PubMed: 7576655]

17. Aoki F, Sakai S & Kohmoto K Regulation of flagellar bending by cAMP and Ca^{2+} in hamster sperm. Mol. Reprod. Dev. 53, 77–83 (1999). [PubMed: 10230819]

18. Espinosa Fet al.Mouse sperm patch-clamp recordings reveal single Cl^{-} channels sensitive to niflumic acid, a blocker of the sperm acrosome reaction. FEBS Lett. 426, 47–51 (1998). [PubMed: 9598976]

19. Kobori H, Miyazaki S & Kuwabara Y Characterization of intracellular Ca^{2+} increase in response to progesterone and cyclic nucleotides in mouse spermatozoa. Biol. Reprod. 63, 113–120 (2000). [PubMed: 10859249]

20. Perez GIet al.Prolongation of ovarian lifespan into advanced chronological age by Bax-deficiency. Nature Genet. 21, 200–203 (1999). [PubMed: 9988273]

21. Arnoult C, Lemos JR & Florman HM Voltage-dependent modulation of T-type calcium channels by protein tyrosine phosphorylation. EMBO J. 16, 1593–1599 (1997). [PubMed: 9130704]

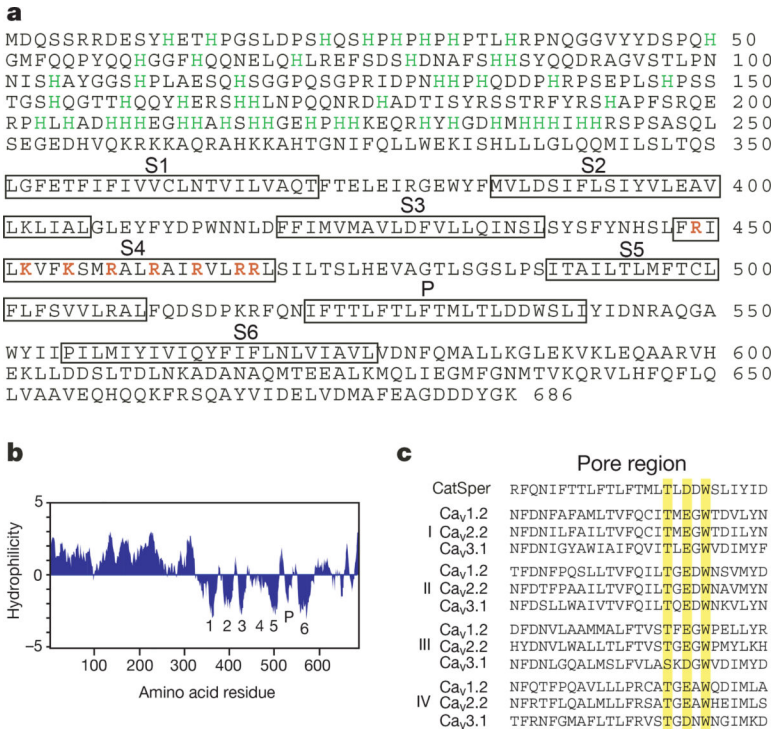

Figure 1.

Primary structure of mouse CatSper. **a**, Amino-acid sequence; the six putative transmembrane domains (S1–S6) and the pore (P) region are boxed. The positively charged amino acids (K/R) in the S4 region are shown in red. Histidines in the first 250 amino acids are labelled in green. **b**, Hydropathy plot of CatSper predicts six transmembrane domains (1–6) and a P loop (P). Window size is 11. **c**, Alignment of the putative pore region of CatSper with that of the four domains (I, II, III, IV) from Ca_V1–3. The conserved residues in the T/S-x-E/D-x-W motif are shaded. GenBank accession numbers: X15539, $Ca_V1.2$; M94172, $Ca_V2.2$; 054898, $Ca_V3.1$; mouse CatSper, AF407332; human CatSper, AF407333.

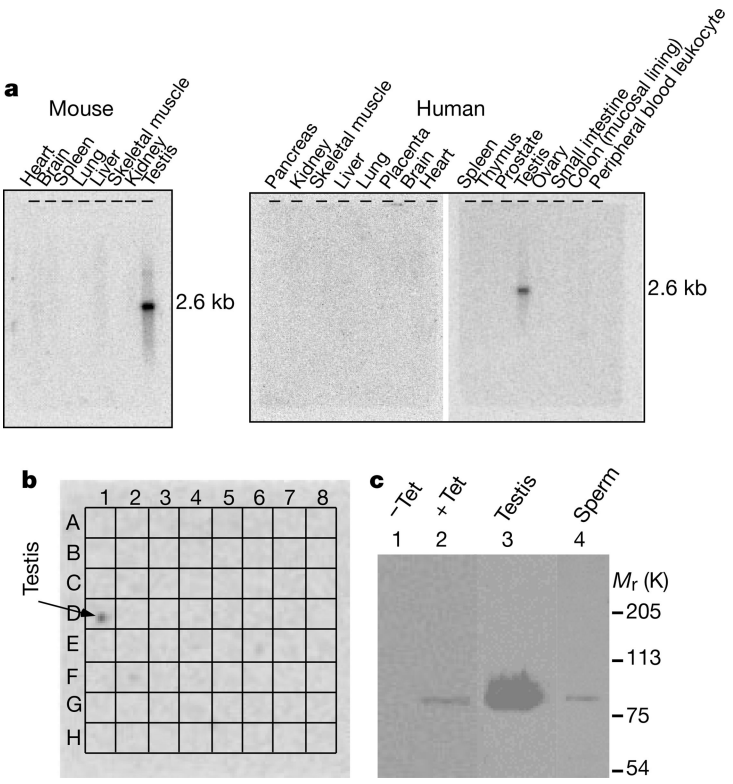

Figure 2.

The restricted expression pattern of CatSper in testis. **a**, Northern blot from mice (left) and human (right) organs. **b**, Dot blot of mRNAs from 50 human tissues (grid superimposed). The tissues in the blot are from left to right: row A, whole brain, amygdala, caudate nucleus, cerebellum, cerebral cortex, frontal lobe, hippocampus, medulla oblongata; row B, occipital lobe, putamen, substantia nigra, temporal lobe, thalamus, nucleus accumbens, spinal cord; row C, heart, aorta, skeletal muscle, colon, bladder, uterus, prostate, stomach; row D, testis, ovary, pancreas, pituitary gland, adrenal gland, thyroid gland, salivary gland, mammary gland; row E, kidney, liver, small intestine, spleen, thymus, peripheral leukocyte, lymph node, bone marrow; row F, appendix, lung, trachea, placenta; row G, fetal brain, fetal heart, fetal kidney, fetal liver, fetal spleen, fetal thymus, fetal lung; and row H, negative controls. **c**, Western blot of CatSper protein. Lanes 1 and 2 were loaded with total protein from HEK-293 cells stably expressing inducible CatSper without (−Tet) and with (+Tet) tetracycline induction. Lanes 3 and 4 were loaded with testis membrane protein and sperm total protein, respectively. M_r, relative molecular mass.

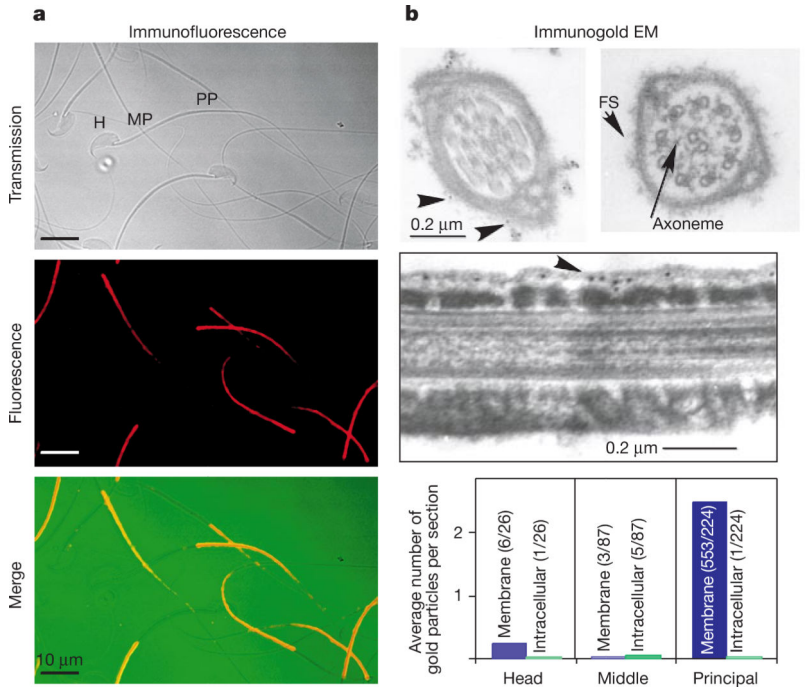

Figure 3.

Localization of CatSper to the plasma membrane of the principal piece of sperm. **a**, Immunostaining of mouse sperm. Top, phase contrast. The head (H), midpiece (MP) and principal piece (PP) regions of the sperm are indicated. Middle, immunofluorescence. Bottom, merged signal where immunofluorescence is labelled red and transmission green. **b**, Sperm immunogold-labelled electron microscopy. Top left, cross-section through the principal piece; arrows indicate gold particles. Top right, fibrous sheath (FS). Middle, longitudinal section. The immunoreactive gold particles are at the cell membrane cytoplasmic face. Bottom, distribution of gold particles along the sperm head, midpiece and principal piece. Gold particles located outside the fibrous sheath were counted as being membrane localized, and inside the fibrous sheath as intracellular. The numbers of sections counted and particles detected are indicated in parentheses.

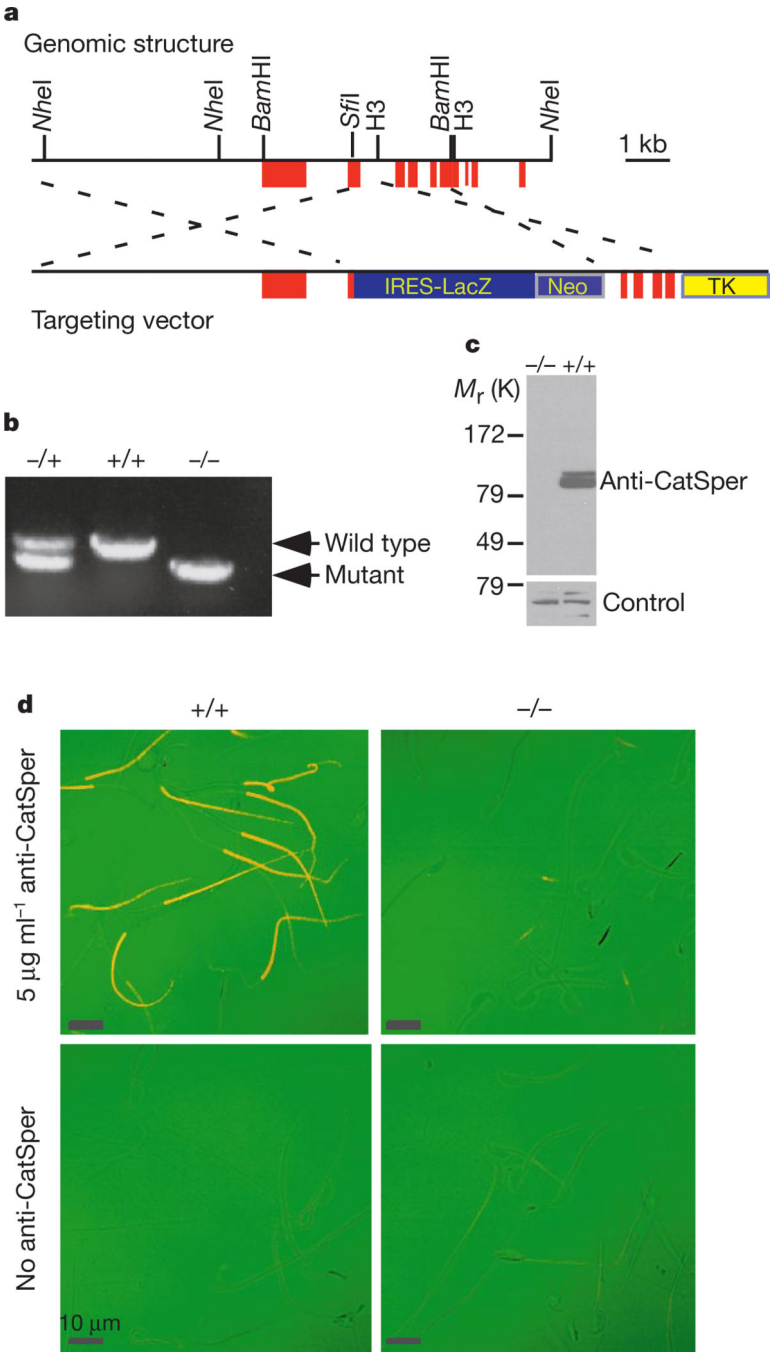

Figure 4.

Targeted disruption of CatSper. **a**, Partial genomic structure of mouse CatSper and targeting vector. Filled red boxes, exons; thin lines, introns. **b**, PCR genotyping confirmed gene disruption. Tail genomic DNA was amplifed with primers specifc for CatSper$^{+/+}$ and CatSper$^{-/-}$. **c**, CatSper protein was absent in mutant mice by western blot. Roughly equal amounts of membrane protein from wild-type and mutant testes were blotted with anti-CatSper antibody. An unrelated antibody controlled for equal protein loading. **d**, Immunostaining of wild-type (+/+) and mutant (−/−) sperm. Primary antibody was omitted

in the control. The transmission signal is green, immunofluorescence is red, and overlap is orange.

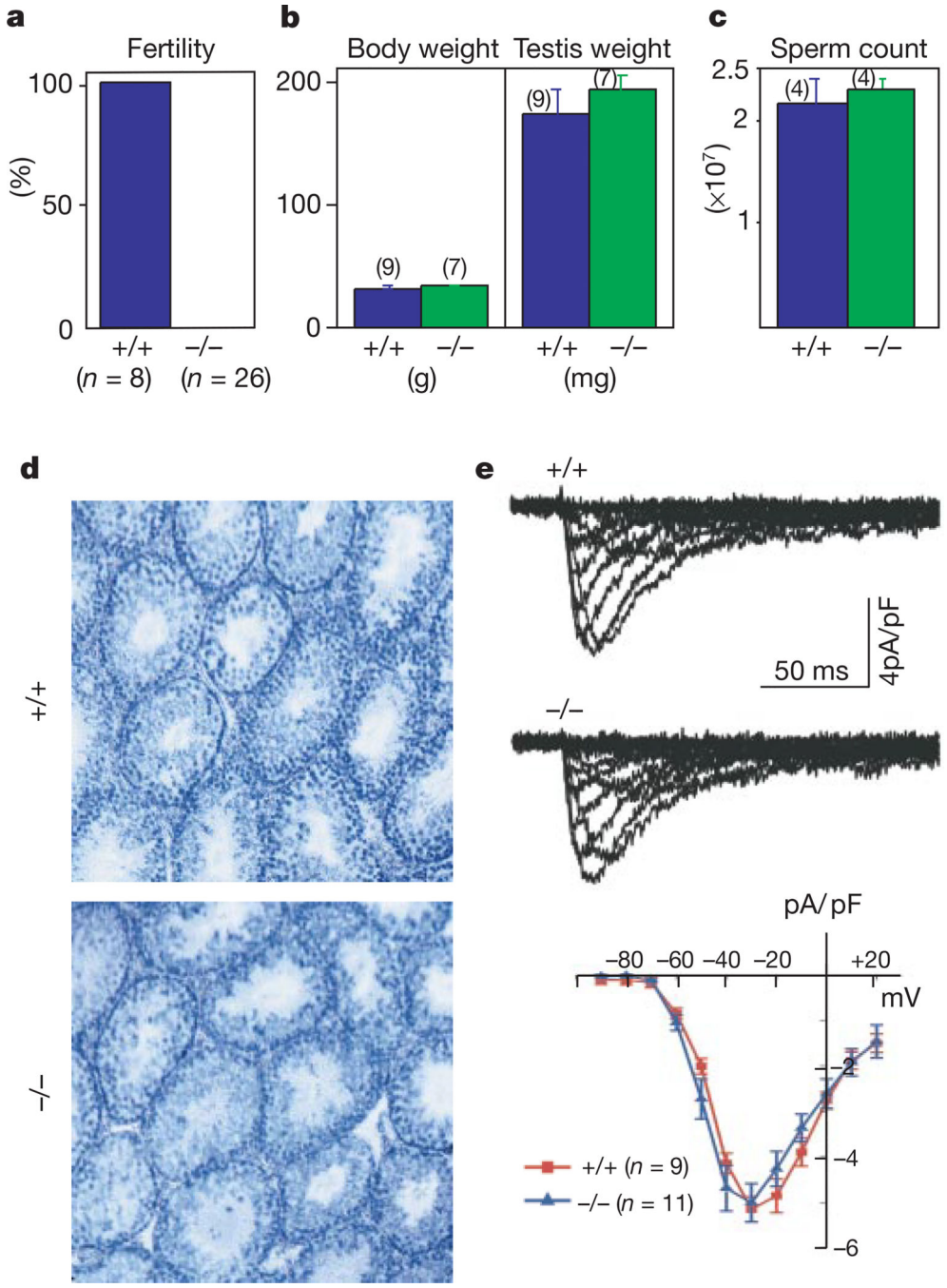

Figure 5.

Male infertility caused by CatSper disruption. **a**, Fertility of CatSper$^{+/+}$ and CatSper$^{-/-}$ males. **b–d**, Mice body and testis weight (**b**), sperm count (**c**), and testis histology (**d**) were not significantly different. Testes sections were stained with haematoxylin/eosin in **d**. **e**, Ca^{2+}-channel currents were indistinguishable between wild-type (+/+) and mutant (−/−) spermatocytes in range of activation, amplitude and kinetics. Currents were elicited by test pulses from −90 to +20 mV (Δ10 mV). Bottom, averaged *I/V* relationships of inward

currents. The holding potential was −100 mV; the average cell capacitances were 10.8 ± 1.4 pF (+/+; $n = 9$) and 12.9 ± 0.9 pF (−/−; $n = 11$).

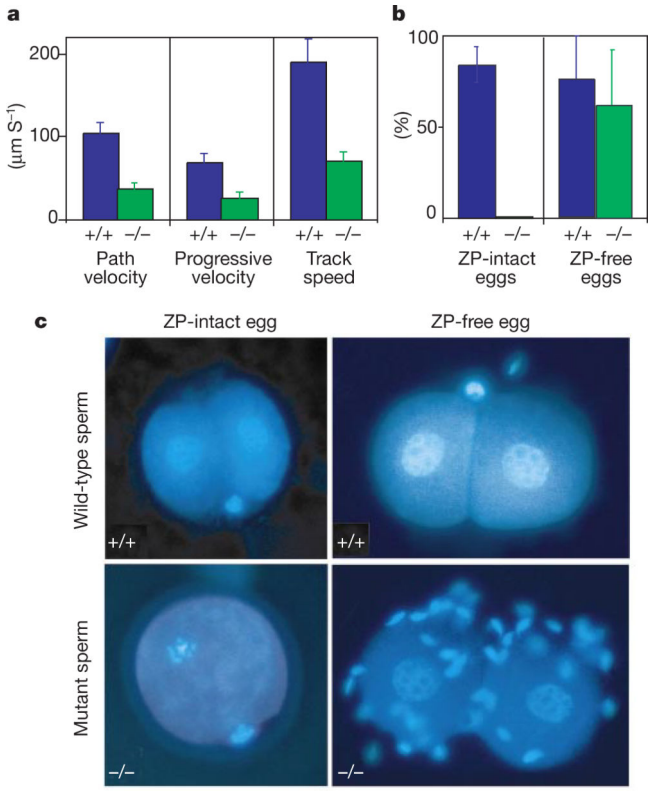

Figure 6.

CatSper$^{-/-}$ sperm motility and *in vitro* fertilization defects. **a**, Quantified sperm motility: path velocity, progressive velocity and track speed. **b**, *In vitro* fertilization (IVF) rates of mutant and the wild-type sperm with zona pellucida (ZP)-intact and ZP-free eggs (three pairs of mutant and wild-type mice each). **c**, Eggs with and without the ZP were incubated with CatSper$^{+/+}$ or CatSper$^{-/-}$ sperm. After 24 h, cells were stained with Hoechst 33342 for chromatin analysis. Note the decondensed chromatin in the two nuclei of the individual blastomeres at the two-cell stage.

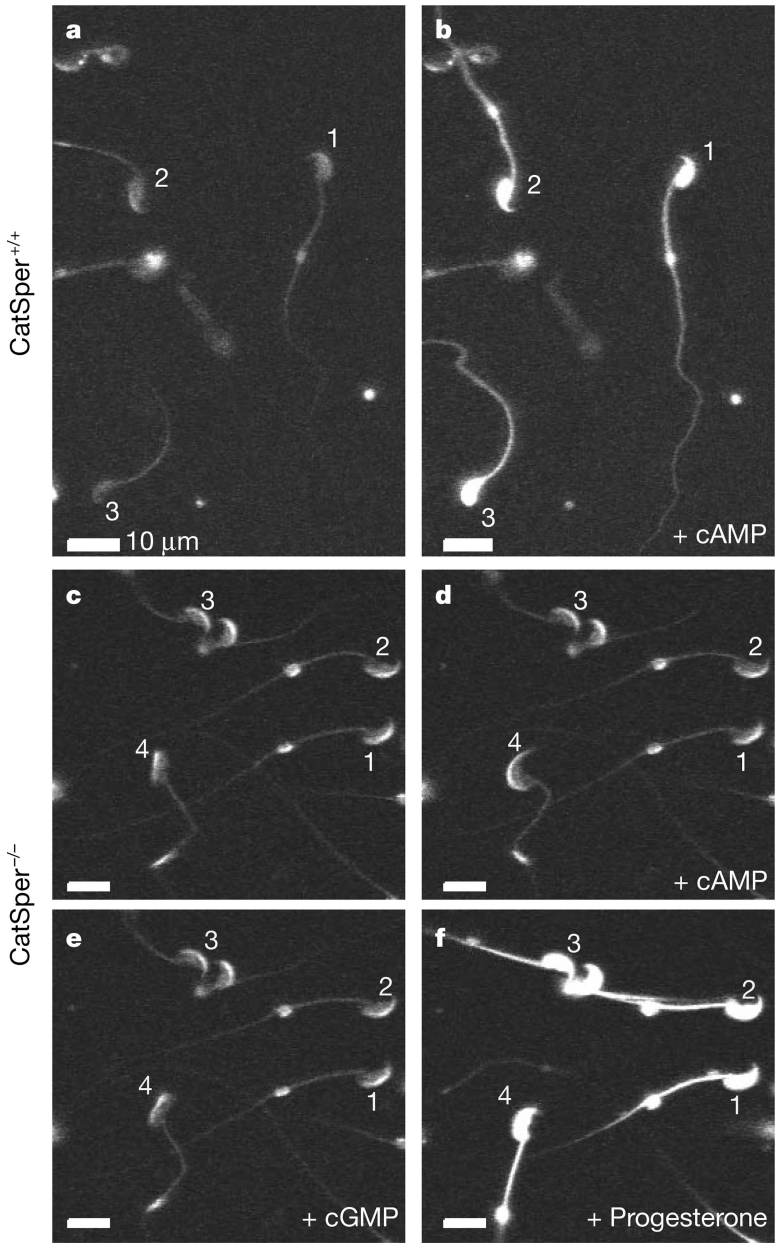

Figure 7.

cAMP-induced calcium influx defect in CatSper$^{-/-}$ sperm. **a**, **b**, Fluo-4 fluorescence images of wild-type sperm before (**a**) and after (**b**) addition of 1 mM cell-permeant cAMP (8-Br-cAMP). **c–f**, Incubation in cell-permeant cAMP (1 mM) or cGMP (1 mM) for 10 s did not induce Ca^{2+} influx in mutant (CatSper$^{-/-}$) sperm. Progesterone (~1 mM), which was used as a positive control for Ca^{2+} responses, initiated a large Ca^{2+} increase in both mutant (**f**) and control (not shown) sperm. Numbers identify individual spermatozoa.

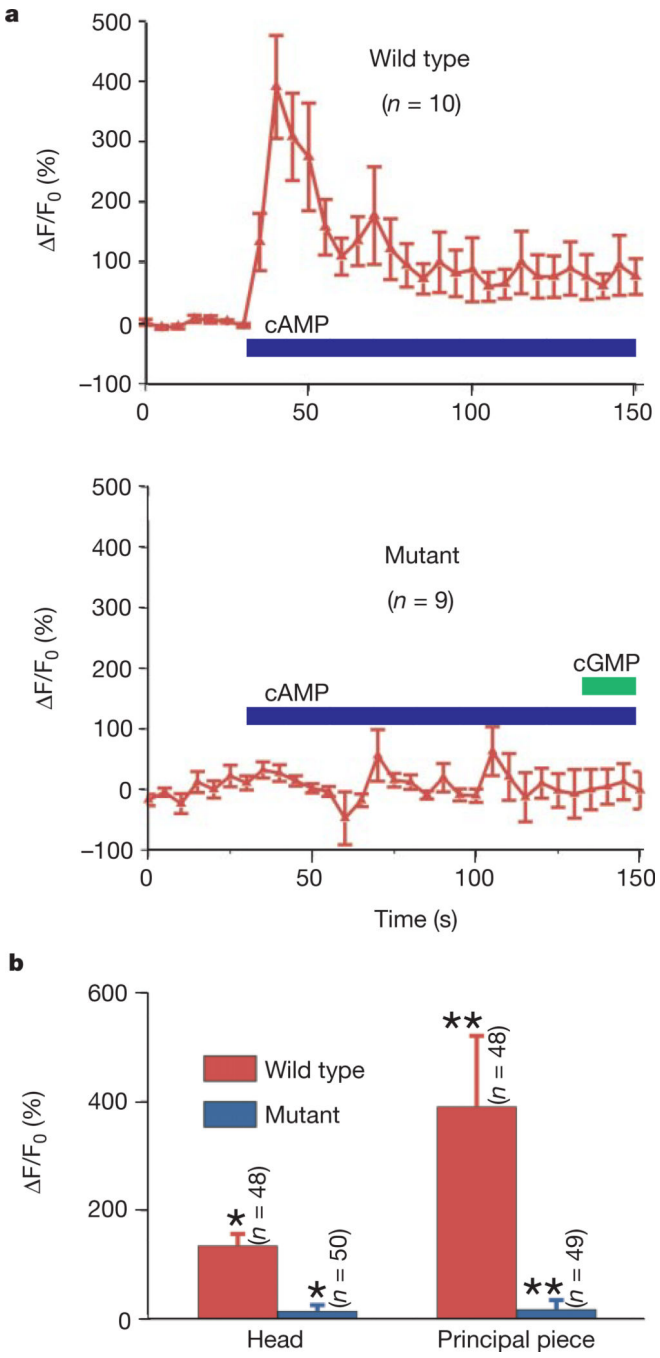

Figure 8.

Summary of cyclic-nucleotide-induced Ca^{2+} changes. **a**, Time courses of cAMP-induced Ca^{2+} changes in the principal pieces of wild-type ($CatSper^{+/+}$) and mutant ($CatSper^{-/-}$) sperm. **b**, Mean fluorescence change in sperm heads and principal pieces from $CatSper^{+/+}$ and $CatSper^{-/-}$ mice. Fluorescence was normalized to the average of the first seven sampling points of the pre-stimulation trace. $^{**}P<0.005$; $^{*}P<0.001$; indicating statistical significance.